Soft Iron/Silicon Composite Tubes for Magnetic Peristaltic Pumping: Frequency-Dependent Pressure and Volume Flow

*Roland Fuhrer, Christoph M. Schumacher, Martin Zeltner, and Wendelin J. Stark**

The combination of force and flexibility enables controlled and soft movements. In sharp contrast, presently used machines are solid and mostly based on stiff driveshafts or cog wheels. Magnetic elastomers are realized through dispersion of small particles in polymer matrices and have attracted significant interest as soft actuators for controlled movement or conveying and are particularly attractive candidates for magnetic pump applications. At present, low magnetic particle loading and thus limited actuator strength have restricted the application of such materials. Here, the direct incorporation of metal microparticles into a very soft and flexible silicone and its application as an ultra-flexible, yet strong magnetic tube, is described. Because metals have a far higher saturation magnetization and higher density than oxides, the resulting increased force/volume ratio afforded significantly stronger magnetic actuators with high mechanical stability, flexibility, and shape memory. Elliptical inner diameter shape of the tubing allowed a very efficient contraction of the tube by applying an external magnetic field. The combination of magnetic silicone tubes and a magnetic field generating device results in a magnetic peristaltic pump.

1. Introduction

Magnetically active, soft polymers have been developed as a potential approach to the realization of movement, as actuators in the fields of microengineering or in biomedicine. These materials are typically based on composites[1–8] consisting of magnetic micro- or nanoparticles dispersed in a polymer matrix[9–12] to provide the desired mechanical properties (stiffness, shape memory, or 3D elasticity).

Magnetic silicones have been investigated for controlled movement[13] or conveying[14] and are particularly attractive candidates for magnetic pump applications. Depending on the specific implementation, anisotropic or isotropic shape changes can be induced in silicone-based composites through the application of an external magnetic field.[15–18] Actuator strength is a direct result of the magnetic particle content (particles mass per volume) and the particle saturation magnetization (force per particles mass). Metallic cobalt[19,20] or iron[21] particles would combine the highest saturation magnetization and high density. High particle loading, however, remains in direct competition with an unwanted increase in brittleness due to particle agglomeration and accompanying loss of flexibility. This fact might be a reason why current micropumps are still constructed by solid and stiff permanent magnets.[18,22] Magnetic peristaltic pumps made of soft, magnetic tubings are rare. Recent studies have shown new roller free[23] or rotating motor with magnetic disc[24] approaches. The major disadvantages of these displacement pumps are time dependent abrasion due to the mechanical workload of the tubing and the relatively high wall shear stress from the continuous displacement of the liquid within the tube[25] (see Supporting Information, Figure S1). Inspired by the skeletal-muscle pumps that aid in the blood circulation by venous contraction,[26,27] a new flexible and highly magnetic active tube was designed to overcome these unfavorable issues. Venous contractions cause a sufficiently large pressure change to create a vacuum that draws blood which is then pumped towards the heart by the following contraction (see Supporting Information, Figure S2). The medically well accepted material polydimethylsiloxane (PDMS)[28,29] was used as a soft and flexible polymer matrix for the present study. In order to directly incorporate metal particles into the bulk polymer, carbonyl iron microparticles were used. We demonstrate the successful incorporation of up to 75 wt% metal particles in silicone, resulting in stable, flexible and homogeneous magnetic composites. In order to demonstrate the application of iron doped silicone tubes as a magnetic pump, a magnetic peristaltic pump similar to the skeletal-muscle pump was designed and operated. A computer simulation of the developed magnetic pump resulted in laminar flow behavior and a maximum shear stress of 290 Pa. Our study demonstrates the reliable use of soft and flexible magnetic silicones for the preparation of peristaltic pumps with low shear stress and without any moving parts, potentially useful for the pumping of sensitive fluids, such as blood.

Dr. R. Fuhrer, C. M. Schumacher, M. Zeltner,
Prof. W. J. Stark
ETH Zurich Institute for Chemical and Bioengineering
Wolfgang-Pauli-Str. 10, HCI E 107
CH-8093 Zurich, Switzerland
E-mail: wendelin.stark@chem.ethz.ch

DOI: 10.1002/adfm.201203572

2. Results and Discussion

2.1. Particle Characterization

The particle size was evaluated by visual particle counting of electron microscopy images and resulted in a mean particle size

© 2013 WILEY-VCH Verlag GmbH & Co. KGaA, Weinheim

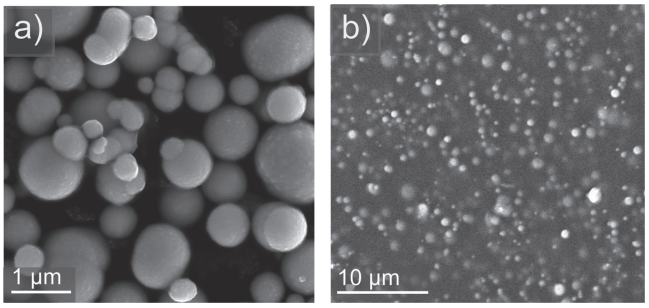

Figure 1. a) SEM images of carbonyl iron microparticles. b) SEM images of cross sections of silicone containing 67 wt% iron particles with respect to polymer indicating a homogenous distribution of embedded particles within the silicone matrix.

of about 1.5 µm for carbonyl iron microparticles (**Figure 1**a). These values are in good agreement with the provided data from the manufacturer (2 µm). Elemental analysis showed metallic contents of 98.6% iron, and underline the metallic core characteristics. The high saturation magnetization of metallic iron microparticles (205 ± 5 emu/g) was confirmed by vibrating sample magnetometer (VSM; see Supporting Information, Figure S3).

2.2. Synthesis of Magnetic Silicone

The magnetic bulk silicone was prepared by dispersing 50 wt% of iron particles, in silicone prepolymer with the aid of a dual asymmetric centrifuge. A transparent crosslinking agent (40 wt% with respect to prepolymer) was used to control the flexibility and mechanical stability of the magnetic silicone. The final low viscous silicone mixture was poured into cylindrical glass casting molds. The obtained magnetic silicone was investigated regarding the homogeneity of particle distribution. Iron embedded silicone showed no visible structuring and smooth surface in scanning electron microscopy (SEM) indicating that the iron microparticles were well distributed within the silicone matrix (Figure 1b). The spherical shape and the particle size confirm the chemical stability of the metal micromagnets throughout the preparation and polymerization process. The entire greyish material was soft and highly flexible with exceptional shape memory even after severe stress.

To benefit from the high saturation magnetization, a high content of micromagnets is required, while keeping the characteristic mechanical properties (softness and flexibility) of the bulk silicone. To find the optimal parameters (i.e., the amount of incorporated iron), a bottom-up approach was used by increasing the particle content step-wisely from 50 to 75 wt%. The final polymer mixtures were placed in two different types of casting molds (polyether ether ketone, PEEK). To facilitate anisotropic contraction effects, the mold was equipped with a removable PEEK filler one of circular and another one with elliptical shape.

The reaction to an applied electromagnetic field showed a very fast and reversible movement towards the magnet. Interestingly, the tubes with a circular inner diameter were only slightly

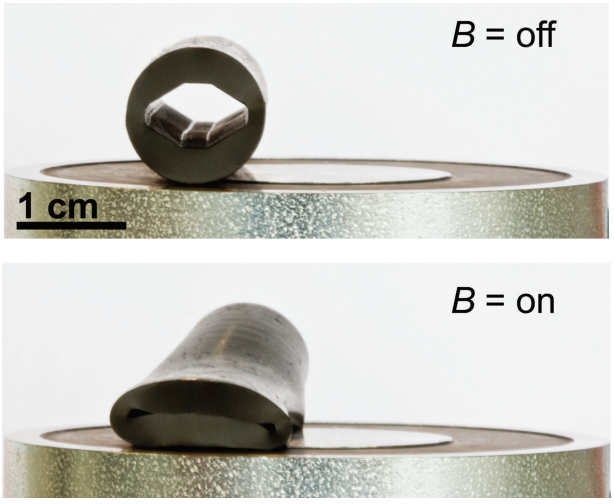

Figure 2. Contraction of a magnetic silicone (67 wt% iron particles) placed on an electromagnet. Without a magnetic field the elliptical shape of the inner diameter is clearly visible (top). Turning the electromagnet on, the magnetic tube contracts by a movement of the upper part of the tube towards the magnet.

or not deformable at all, independent of the iron amount. In contrast, the inner diameter of elliptical shape promoted a fast and complete contraction of the magnetic tubing (**Figure 2**) due to the smaller resilience of the thinner tube wall of the elliptic shape. Silicones with 67 wt% metallic iron and elliptical inner diameter could be entirely contracted within several 100 ms using a simple electromagnetic coil (0.43 T). VSM measurements underlined this magnetic field responsive behavior as the saturation magnetization of the composite was only reduced to 133 ± 2 emu/g (35% reduction compared to pure iron). Tubes with higher microparticle content than 67 wt% were already too stiff and, thus, prevented a fast contraction.

2.3. Magnetic Field Driven Peristaltic Pumping

In order to evaluate possible applications as soft magnetic actuators or magnetic peristaltic pumps, four magnetic silicone tubes of 8 cm length and 1.2 cm outer diameter were connected to one long tube. As joints, in-house made hollow elliptically formed PEEK parts were used and sealed with a hose clamp. This assembled pipe was placed on a magnetic field generating in-house designed device made of four solenoids (**Figure 3**). The solenoids were fixed on aluminum plates to compensate the generated heat. For long term use (several hours) the plate with additional pedestals was positioned in an ice bath (operating temperature < 20 °C). The power supply was controlled with a personal computer running a LabVIEW program which allowed, by simple button activation, the control of the respective solenoid for a specific time. This easy handling gave access to study different pump patterns with different contraction times, i.e., the activated time of solenoids. Requirements for the patterns were unidirectional flow and maximum flow rates. Therefore, two different contraction methods (**Scheme 1**), a fast with partially activated parts of the tubes and another slow and

© 2013 WILEY-VCH Verlag GmbH & Co. KGaA, Weinheim

Figure 3. Final apparatus of a magnetic peristaltic pump. Four magnetic tubes were connected to each other and placed on top of 4 solenoids. Tubes were positioned at the edge of the field generating pillar because of the high magnetic field at this position (0.43 T). Turning the electromagnets on, the tube showed a clear contraction towards the magnet and allowed pulsatile movement.

entirely contracted tube, were investigated in more detail. At different contraction times the flow rate and maximum hydrostatic back-pressure were evaluated (5 times, **Figure 4**) and resulted with pattern 1 in 78.5 ± 1 mL/min at a maximum back-pressure of 4.12 ± 0.03 kPa with a contraction interval of 250 ms. The slower pattern (pattern 2) was notably poorer with a maximum flow of 48.3 ± 1 mL/min at a possible back-pressure of 3.27 ± 0.04 kPa. A possible explanation might be the technical boundaries of the power supply. For safety reasons the maximum current was set to 2.6 A. When all solenoids were activated at the same time this value was reached immediately and hindered the generation of a maximum magnetic field in each solenoid. This underlines the advantage of a partially activated tube especially when better pump properties could be attained with this setup (pattern 1).

A minor disadvantage of pattern 1 could be some backflow in the region between the magnets. In fact a backflow was not observed when the lighting part of the tube was taken out of the reservoir to count any backflow droplets. In the case of pattern 2 there is no backflow and mixing expected and observed, as the whole pump was squeezed one by one until complete contraction of the pump.

Roller pumps usually comprise several rotating rollers that peristaltically treat the tubing. This action, the tube squeezing, gently propels the liquid through the tubing. As the liquid is pushed in front of a roller (see Supporting Information, Figure S1), relatively high wall shear forces occur.[25] This shear forces may become disadvantageous when sensitive liquids, such as blood, are pumped. The presented magnetic pumping action is considered to be superior to the action of the roller pump because of the static conveying form (see Supporting Information, Figure S2). In contrast to currently used pumps, the major advantage of the pump presented here, is the self-induced contraction of the magnetic tube, i.e., no external moving parts are needed. This allows a skeletal-muscle

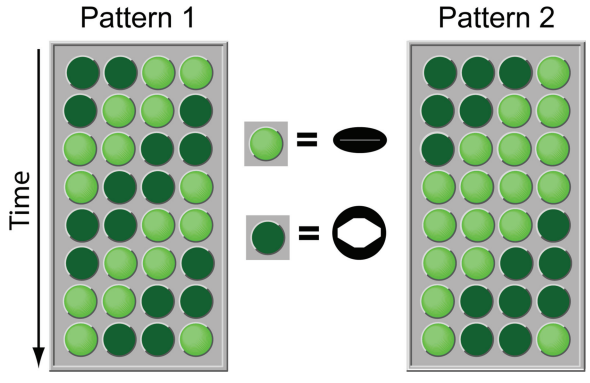

Scheme 1. Programmed LabVIEW pattern for two different pump settings. LabVIEW was running row by row (contraction time, the activated time of a solenoid) through the program with a loop function. Bright buttons means activated magnetic field and, thus, a contraction of the magnetic tube occurred and a pulsatile pump action took place. Pattern 1 was a fast and partially activated pattern (2 complete passes) where pattern 2 was relatively slow.

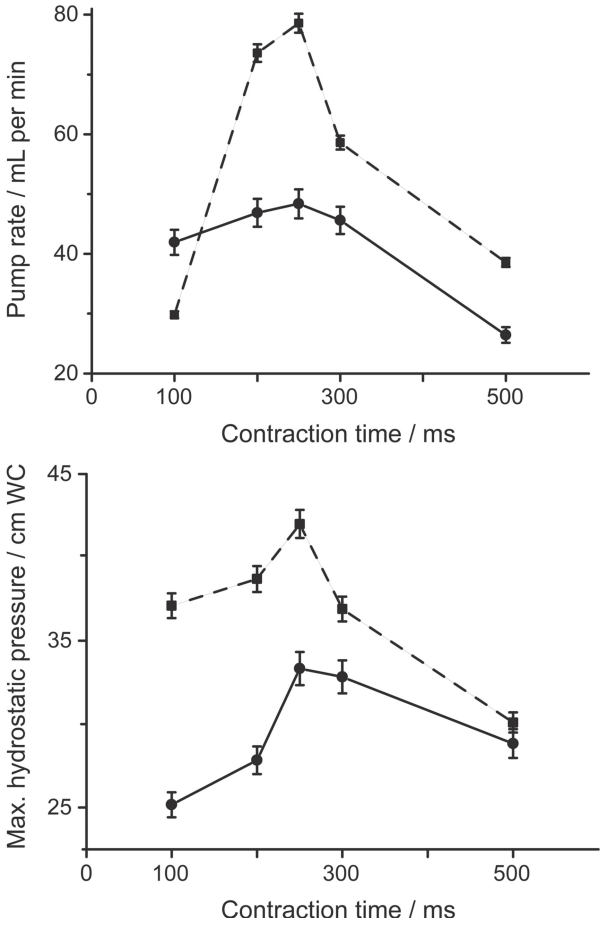

Figure 4. Pump performance as a function of pump pattern and contraction time. Dashed line: pattern 1; solid line: pattern 2. Varying the contraction time from 100 to 500 ms demonstrated a maximum performance at 250 ms with both patterns. Maximum flow rate was measured with pattern 1 at 78.5 mL min^{-1} with a back-pressure of 4.1 kPa.

© 2013 WILEY-VCH Verlag GmbH & Co. KGaA, Weinheim

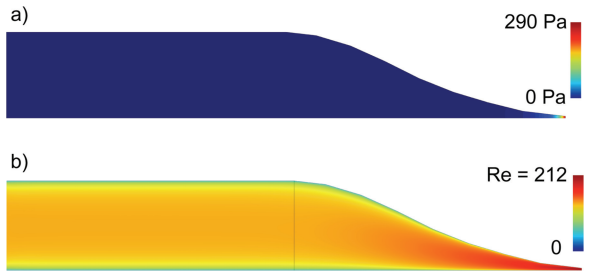

Figure 5. Initial shear stress (top) and Reynolds number distribution (bottom) simulated with COMSOL Multiphysics during contraction resulted in a maximum shear stress of 290 Pa and a Reynolds number of 212 in the region of contraction.

pump-like pumping with relatively low shear stress and a controlled smooth contraction by adjusting the magnetic field. To evaluate the shear stress, a computer simulation with COMSOL Multiphysics was performed and demonstrated a maximum shear stress of 290 Pa (**Figure 5**). The high shear stress was mainly observed in the almost fully contracted tube region and decreased very fast when the tube was in elongated position. The typical maximum shear stress range found in roller pumps varies from 920 to 940 Pa.[25] The obtained simulated maximum and minimum Reynolds number (large and small diameter as characteristic lengths) of 212 and 43, respectively, demonstrate that laminar flow is predominant in the present setting. This interesting fact paired with low shear stress characterizes the soft contraction behavior of the present magnetic peristaltic pump. The present magnetic pump may be operated at a low risk of damaging sensitive fluids.

3. Conclusion

Carbonyl iron metal microparticles have enabled the preparation of magnetic silicones that combine the use of the highest possible saturation magnetizations (pure metallic iron) and high particle loading of up to 75 wt% with respect to polymer without negatively affecting mechanical stability and integrity. The optimal particle amount for the application as soft, magnetic pump (mechanical stability and flexibility) is about 67 wt%. A computer based simulation of the contracted tube showed lower shear stress compared to existing roller pump simulation. These properties allowed the design and production of a magnetic peristaltic pump without any external moving parts which may facilitate the use of soft silicone tubing in blood pumps, heart pump components or micropumps. Magnetic field driven pumps may eventually pave the way to develop location independent pumps i.e. having the electrical parts of a pump outside of a protection barrier and the magnetic tubing in a more demanding zone.

4. Experimental Section

Iron carbonyl particles (CIP HQ, BASF) were used as received. The magnetic particles were analyzed by element microanalysis (LECO CHN-900) to acquire quantitative confirmation about the particle composition. The iron particles were further investigated by scanning electron microscopy (SEM, Nova NanoSEM 450, FEI) to obtain the average particle size (100 counts). The magnetic properties were measured by vibrating sample magnetometer (VSM, MicroMag 3900 Vibrating Sample Magnetometer VSM).

Magnetic Silicone Preparation: Appropriate amounts (50 wt%) of iron particles were dispersed in a prepolymer (Neukasil RTV 23, Altropol) using a dual asymmetric centrifuge (SpeedMixer DAC 150 FVZ) with 0.5 min at 1300 rpm, 2 min at 1500 rpm and 5 min at 1800 rpm, respectively. The highly viscous doped silicone was crosslinked with 40 wt% crosslinking agent (VN A7, transparent, Altropol) with respect to prepolymer mass by mixing with the dual asymmetric centrifuge (2 × 5 min at 1800 rpm). The resulting mixture was degassed (7 mbar), poured into a cylindrical casting mold with 5 mm thickness and cured at 50 °C for 60 min, subsequently. The obtained magnetic silicone slices were optically analyzed to recognize any sedimentation of particles.

Synthesis of Magnetic Silicone Tubes with Different Inner Diameter Shapes and Magnet Content: Homogeneous composites containing 50, 60, 67, 71 and 75 wt% of magnetic iron particles with respect to total silicone mass were prepared as described above. The final greyish and low viscous mixture was degassed (7 mbar) to achieve an air bubble free blend before gently pouring into an in-house made casting mold based on polyether ether ketone (PEEK). This casting mold was designed once with a circular inner diameter and another with an inner elliptical diameter to allow easier magnetic force derived deformation of the resulted magnetic silicone tube. Curing was done at 50 °C for 60 min by upside down changes of the mold every 5 min for the first 20 min to avoid sedimentation of the iron particles. Magnetic silicone tubes were investigated by SEM after placing on carbon tape glued to aluminum stubs and were shortly blown up to detect any air bubbles. Magneto-elastic measurements, i.e., entire magnetic contraction tests, were performed at ambient conditions on an electromagnet GMH X050 (Magnet-Schultz, = 24 V, 100% ED) controlled with a programmable power supply (80 V, Voltcraft Plus, PSP1803). VSM measurements were performed with magnetic silicone tubes containing 67 wt% magnetic particles.

Magnetic-Field-Driven Peristaltic Pump: Magnetic pump tests were performed at ambient condition on electromagnets type GMH X050. Four electromagnets were arranged in a line and anchored on an aluminum plate (45 cm × 20 cm × 0.6 cm). Solenoid activities were controlled by a programmable power supply which was connected to a personal computer. Pulsative and peristaltic deformations were obtained using LabVIEW (Version 8.2) by regulating power on/off and contraction time, respectively. The program was such designed that the user can apply desirable pump pattern by activating/deactivating buttons, which represented a specific solenoid. To achieve a higher magnetic force, the solenoids were operated with a 3.4 fold higher voltage (82 V) as designated. The highest field strength used on the pole of the electromagnet was 0.43 Tesla (Gaussmeter, GM-2, AlphaLab Inc.). The generated heat was compensated by placing the aluminum plate with extra pedestals in an ice bath to keep the solenoid temperatures below 20 °C (controlled with an infrared thermometer, Scantemp pro 440). To improve heat transfer of the solenoids towards aluminum plate, the bottom of the solenoids were treated with thermal paste.

The four single magnetic silicone tubes were connected to each other with an in-house made elliptical hollow spool piece made of PEEK and placed onto the in-house developed magnetic field generator. The contractions of the magnetic silicone, i.e., pump activities, were recorded with a digital camera. A representative movie clip is available in the electronic supporting information.

Pumping Properties of the Magnetic Peristaltic Pump: Two different pumping patterns were investigated regarding the maximum pump capacity and back-pressure. The first pattern was a relatively fast movement with just two active solenoids compared to the second one where all four solenoids were activated at the same time. By adjusting the contraction time, i.e., the time of activated electromagnets (100 ms, 200 ms, 250 ms, 300 ms and 500 ms), the pumped volume in one minute was determined by mass using a balance (XS205, Mettler Toledo)

© 2013 WILEY-VCH Verlag GmbH & Co. KGaA, Weinheim

to obtain the pump capacity at the respective time and to investigate the optimal time with the highest capacity. To examine the maximum back-pressure where the pump was still able to pump up water, a water column (WC) was measured after 10 s activated pump time with the aid of a back-flow preventer. Assuming a water temperature of 20 °C the conversion of one cm WC to kPa refers to 0.098.[30]

Fluid Shear Stress and Flow Modeling: A model to describe shear stress and fluid velocity behavior during the contraction of a silicone tube has been developed under the COMSOL Multiphysics finite-element platform (Version 4.3). Due to the numerical constraints of the finite-element method the shear stress distribution was simulated with a small slit between both tube walls, i.e., shortly before the complete closing of the tube during contraction. Therefore the end geometry of the tube contraction was fixed with a very tiny slit but the dynamic fluid throughput was simulated by a plug-flow profile in space (see Supporting Information, Figure S4). A smoothed Heaviside step function in time was used to solve the parameters under the given flow conditions. Reynolds number was calculated using following blood characteristics: density, ρ = 1060 kg/m^3;[31] dynamic viscosity, μ = 0.005 Pa s;[32] rate of flow, v = 0.2 m/s (given by apparatus); large diameter, $l_{c,L}$ = 0.005 m; and small diameter, $l_{c,S}$ = 0.003 m of the tubing.

Supporting Information

Supporting Information is available from the Wiley Online Library or from the author.

Acknowledgements

The authors are grateful to Urs Krebs and Max Wohlwend for magnetic field device construction. The authors thank Prof. Ann Hirt, Institute for Geophysics, ETHZ, for VSM measurements. Financial support by ETH Zurich is kindly acknowledged.

Received: December 3, 2012
Revised: January 25, 2013
Published online: March 6, 2013

[1] L. C. A. Oliveira, R. Rios, J. D. Fabris, V. Garg, K. Sapag, R. M. Lago, *Carbon* **2002**, *40*, 2177.
[2] S. R. Rudge, T. L. Kurtz, C. R. Vessely, L. G. Catterall, D. L. Williamson, *Biomaterials* **2000**, *21*, 1411.
[3] S. L. Peng, M. Y. Zhang, X. Z. Niu, W. J. Wen, P. Sheng, Z. Y. Liu, J. Shi, *Appl. Phys. Lett.* **2008**, *92*, 012108.
[4] A. Fuchs, Q. Zhang, J. Elkins, F. Gordaninejad, C. Evrensel, *J. Appl. Polym. Sci.* **2007**, *105*, 2497.
[5] S. Abramchuk, E. Kramarenko, D. Grishin, G. Stepanov, L. V. Nikitin, G. Filipcsei, A. R. Khokhlov, M. Zrinyi, *Polym. Adv. Technol.* **2007**, *18*, 513.
[6] P. M. Xulu, G. Filipcsei, M. Zrinyi, *Macromolecules* **2000**, *33*, 1716.
[7] M. Zrinyi, L. Barsi, A. Buki, *Polym. Gels Network* **1997**, *5*, 415.
[8] R. Fuhrer, E. K. Athanassiou, N. A. Luechinger, W. J. Stark, *Small* **2009**, *5*, 383.
[9] R. A. Frimpong, S. Fraser, J. Z. Hilt, *J. Biomed. Mater. Res. Part A* **2007**, *80A*, 1.
[10] B. A. Evans, B. L. Fiser, W. J. Prins, D. J. Rapp, A. R. Shields, D. R. Glass, R. Superfine, *J. Magn. Magn. Mater.* **2012**, *324*, 501.
[11] R. T. Olsson, M. Samir, G. Salazar-Alvarez, L. Belova, V. Strom, L. A. Berglund, O. Ikkala, J. Nogues, U. W. Gedde, *Nat. Nanotechnol.* **2010**, *5*, 584.
[12] Y. H. Kim, J. E. Lee, S. K. Cho, S. Y. Park, I. B. Jeong, M. G. Jeong, Y. D. Kim, H. J. Choi, S. M. Cho, *Colloid Polym. Sci.* **2012**, *290*, 1093.
[13] V. Q. Nguyen, A. S. Ahmed, R. V. Ramanujan, *Adv. Mater.* **2012**, *24*, 4041.
[14] S. Shoji, M. Esashi, *J. Micromech. Microeng.* **1994**, *4*, 157.
[15] T. Kimura, Y. Umehara, F. Kimura, *Soft Matter* **2012**, *8*, 6206.
[16] L. Hsu, C. Weder, S. J. Rowan, *J. Mater. Chem.* **2011**, *21*, 2812.
[17] S. H. Xuan, Y. L. Zhang, Y. F. Zhou, W. Q. Jiang, X. L. Gong, *J. Mater. Chem.* **2012**, *22*, 13395.
[18] Y. Zhou, F. Amirouche, *Micromachines* **2011**, *2*, 345.
[19] A. H. Lu, E. L. Salabas, F. Schuth, *Angew. Chem. Int. Ed.* **2007**, *46*, 1222.
[20] R. N. Grass, E. K. Athanassiou, W. J. Stark, *Angew. Chem. Int. Ed.* **2007**, *46*, 4909.
[21] W. C. Jiang, J. J. Yao, X. L. Gong, L. Chen, *Chin. J. Chem. Phys.* **2008**, *21*, 87.
[22] T. R. Pan, S. J. McDonald, E. M. Kai, B. Ziaie, *J. Micromech. Microeng.* **2005**, *15*, 1021.
[23] V. Shkolnikov, J. Ramunas, J. G. Santiago, *Sens. Actuators A.* **2010**, *160*, 141.
[24] M. Du, X. Y. Ye, K. Wu, Z. Y. Zhou, *Sensors* **2009**, *9*, 2611.
[25] J. W. Mulholland, J. C. Shelton, X. Y. Luo, *J. Fluids Struct.* **2005**, *20*, 129.
[26] C. F. Rothe, *J. Appl. Physiol.* **2005**, *99*, 773.
[27] D. Sheriff, *J. Appl. Physiol.* **2005**, *99*, 371.
[28] S. D. Hajdu, N. Agmon-Levin, Y. Shoenfeld, *Eur. J. Clin. Invest.* **2011**, *41*, 203.
[29] D. Stavrou, O. Weissman, E. Winkler, L. Yankelson, E. Millet, O. P. Mushin, A. Liran, J. Haik, *Aesthetic Plast. Surg.* **2010**, *34*, 646.
[30] W. M. Haynes, in *CRC Handbook of Chemistry and Physics 93rd Edition (Internet Version 2013)*, (Ed: W. M. Haynes), CRC Press/Taylor Francis, Boca Raton, FL **2012-2013**.
[31] J. Cutnell, K. Johnson, in *Introduction to Physics*, (Ed: J. Cutnell, K. Johnson), John Wiley and Sons, Ltd., West Sussex, UK **2012**, p. 1072.
[32] J. Harkness, *Biorheology* **1971**, *8*, 171.

© 2013 WILEY-VCH Verlag GmbH & Co. KGaA, Weinheim